The Journal of Experimental Biology 213, 3473-3486

doi:10.1242/jeb.046508

# Evolution of anatomical and physiological specialization in the compound eyes of stomatopod crustaceans

Megan L. Porter[1,*], Yunfei Zhang[1], Shivani Desai[1], Roy L. Caldwell[2] and Thomas W. Cronin[1]

[1]Department of Biological Sciences, University of Maryland Baltimore County, Baltimore, MD 21250, USA and [2]Department of Integrative Biology, University of California, Berkeley, CA 94720, USA

*Author for correspondence (porter@umbc.edu)

Accepted 26 July 2010

## SUMMARY

**Stomatopod crustaceans have complex and diverse visual systems. Among their many unique features are a specialized ommatidial region (the midband) that enables the eye to have multiple overlapping visual fields, as well as sets of spectral filters that are intercalated at two levels between tiers of photoreceptors involved in polychromatic color vision. Although the physiology and visual function of stomatopod eyes have been studied for many years, how these unique visual features originated and diversified is still an open question. In order to investigate how stomatopods have attained the current complexity in visual function, we have combined physiological and morphological information (e.g. number of midband rows, number of filters in the retina, and the spectral properties of filters) with new phylogenetic analyses of relationships among species based on nucleotide sequence data from two nuclear (18S and 28S rDNA) and two mitochondrial [16S and cytochrome oxidase I (COI)] genes. Based on our recovered phylogenetic relationships among species, we propose two new superfamilies within the Stomatopoda: Hemisquilloidea and Pseudosquillodea. Maximum likelihood ancestral state reconstructions indicate that ancestral stomatopod eyes contained six midband rows and four intrarhabdomal filters, illustrating that the visual physiological complexity originated early in stomatopod evolutionary history. While the two distal filters contain conservative sets of filter pigments, the proximal filters show more spectral diversity in filter types, particularly in midband row 2, and are involved in tuning the color vision system to the photic environment. In particular, a set of related gonodactyloid families (Gonodactylidae, Protosquillidae, Takuidae) inhabiting shallow, brightly lit coral reef waters contain the largest diversity of filter pigments, which are spectrally placed relative to the underlying photoreceptors to take advantage of the broad spectrum of light available in the environment.**

Key words: Stomatopoda, visual complexity, filters, physiology, eye evolution, phylogeny, character reconstruction.

## INTRODUCTION

The stomatopod crustaceans, or mantis shrimps, are among the most charismatic of animals. While these marine creatures have many unusual and interesting biological characteristics, they are best known for their spectacular visual systems. These feature multiple overlapping visual fields in each eye, polychromatic color vision, numerous ultraviolet-sensitive spectral channels, as well as linear and circular polarization vision (see Horridge, 1978; Marshall, 1988; Cronin and Marshall, 1989a; Cronin and Marshall, 1989b; Marshall et al., 1991a; Marshall et al., 1991b; Marshall and Oberwinkler, 1999; Cronin and Marshall, 2004; Chiou et al., 2008). Underlying these functional capabilities are several anatomical and molecular specializations, including the greatest spectral and molecular diversity of visual pigments yet described in a single retina (Porter et al., 2009).

Systems of color vision in most animals are based on relatively few – typically two to five – spectral photoreceptor classes. One reason for this is that the number of functionally independent types in a given visual system is limited by the relatively broad absorption bandwidths of typical visual pigments (Barlow, 1982). The retinal design of many stomatopod species enables the multiplication of spectral classes by placing receptors devoted to color vision in tiers, allowing the visual pigments of distal tiers to act as filters for the proximal tiers, and by incorporating a series of photostable spectral filters within a subset of the rhabdomeric photoreceptors (Marshall, 1988; Marshall et al., 1991a; Marshall et al., 1991b). Such organization is possible because stomatopod eyes are regionally specialized. Except in deep-sea species, their apposition compound eyes are divided into two roughly ovoid or hemispherical ommatidial arrays that make up the dorsal and ventral halves of each eye. These extended peripheral arrays are separated by an equatorial region termed the midband, constructed from two, three or six parallel rows of ommatidia (Fig. 1). Ommatidia making up the two-row or three-row midbands are not obviously different from those throughout the rest of the eye but in six-row midbands, ommatidia of the four most dorsal rows, which are thought to be involved in color vision, include the serial tiering and filtering mentioned above. Even here, however, there is extensive variation among species, most obviously in the number of filter types included and the spectral classes of filters used (see Fig. 2) (Manning et al., 1984a; Manning et al., 1984b; Marshall et al., 1991b; Cronin et al., 1994b; Ahyong and Harling, 2000; Harling, 2000).

Most stomatopod species with six-row midbands have four anatomically distinct intrarhabdomal filter classes, i.e. two in the second midband row and two in the third (the first and fourth rows of the midband, which are also tiered and are thought to be involved in color vision, never have filters). In these species, each of the two rows has a distal filter type separating the ultraviolet-sensitive eighth retinular cell at the top of the rhabdom from a receptor tier constructed from a subset of the seven main retinular cells (R1–R7), plus a proximal filter type at the junction of this receptor tier with a final tier including the remaining cells from the R1–R7 set. While

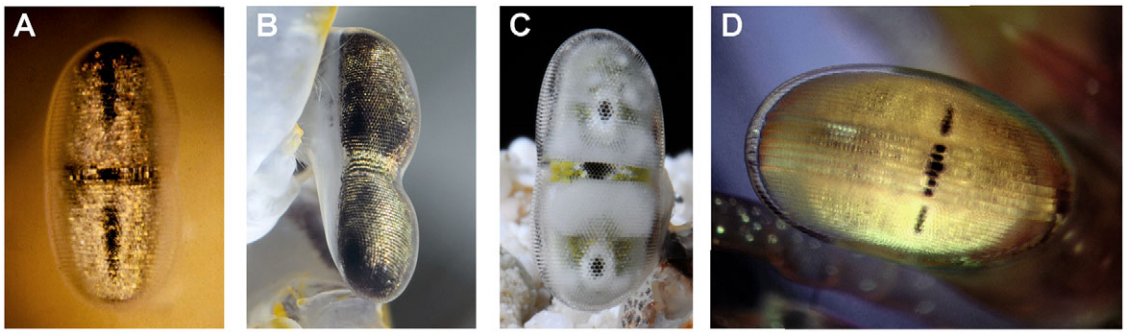


Fig. 1. Photographs of stomatopod eyes to show variation in the midband organization. All eyes are shown with dorsal upwards. (A) Squilloid eye with two midband rows (*Squilla empusa*; photo by T.W.C.). (B) Parasquilloid eye with three midband rows (*Pseudosquilliopsis marmorata*; photo by R.L.C.). (C) Lysiosquilloid eye with six midband rows (*Lysiosquillina sulcata*; photo by R.L.C.). (D) Gonodactyloid eye with six midband rows (*Neogonodactylus bredini*; photo by M. Bok).

the distal and proximal filters in the second row occasionally have identical spectral absorption, in most species they are spectrally distinct; the filters in the third ommatidial row are always different from each other and from either of the second row types (Cronin et al., 1994b). These photostable filters are spectrally offset from the visual pigments of the underlying tiers, producing well-tuned receptor sets for the polychromatic color vision system (Cronin and Marshall, 1989a; Cronin and Marshall, 1989b; Cronin et al., 1994c). However, a number of species of stomatopods with six-row midbands show a different filter organization from that just described. Species may lack up to two filter classes, specifically the proximal types in the second and/or third row (Fig. 2).

Thus, the retinas of modern stomatopod species exhibit a puzzling pattern of diversity in the complexity of the midband, in the variety of spectral types of intrarhabdomal filters used and even in the number of filter types in a single retina. Some types of filters, such as the distal class in the second ommatidial row, seem to be quite consistent across many stomatopod species, showing little variation throughout the group as a whole (Cronin et al., 1994b). Others, for example the proximal filter type in this same row (when present), can be extremely variable among species. Some filter classes (particularly in the third row) show notable variability even among closely related species. A final level of complexity is added in some species, which can replace some filter classes with others when the photic environment changes (Cronin et al., 2001; Cheroske and Cronin, 2005; Cheroske et al., 2006). All of these specializations produce visual systems that are functionally diverse and physiologically competent (Cronin and Marshall, 2004; Marshall et al., 2007).

Understanding the evolutionary history that has produced the current anatomical and physiological diversity presents a difficult problem. For example, is the two-row midband a primitive design, ancestral to six-row types or does it result from a loss of function, perhaps for adaptation to dim, spectrally simple habitats? Similarly, are retinas containing only two or three filter types ancestral to or derived from those with four filters, or is the number of filter classes plastic, simply reflecting the adaptation to different photic environments? Does the spectral diversity of the various filter classes arise from extreme evolutionary lability in the use of the incorporated pigments or is there some systematic pattern in all of this complexity? One way to address these questions is to investigate the evolutionary patterns of particular eye traits in the context of stomatopod species evolution. This method requires both well-characterized physiological data across a range of species and a well-resolved phylogeny of species relationships, upon which the distribution of traits observed in extant species can be used to infer ancestral character states.

Until recently, phylogenies of modern stomatopods were mostly constructed using strictly morphological data, and while these phylogenies were comprehensive (e.g. Ahyong and Harling, 2000), they did not seem to provide reasonable explanations for eye evolution and the origins of the currently seen functional diversity. As one example, the superfamily Gonodactyloidea contains species with only two filter types (e.g. *Hemisquilla californiensis*) but most stomatopods assigned to this superfamily have four filter classes. Similarly, members of the Lysiosquilloidea may have either two or three filter types. Harling noted that aspects of eye design are poorly correlated with standard phylogenies, questioning their validity (Harling, 2000).

Recently, studies have begun to incorporate molecular phylogenetics to examine stomatopod relationships (Barber and Erdmann, 2000; Ahyong and Jarman, 2009). The most recently published work (Ahyong and Jarman, 2009) includes 19 species from a number of morphologically assigned superfamilies, representing excellent overall coverage but with few species in terminal taxa. Based on three genetic loci, this molecular phylogeny differs in many revealing and often significant details from the older morphological trees but the positions of several crucial branches remain ambiguous. Unfortunately, neither of the available molecular phylogenies include more than a few species for which filter absorbance spectral data are available, making it difficult to track the evolution of filter diversity and of individual filter types.

We therefore decided to base our investigation of the evolution of crucial visual features in the Stomatopoda on a new, expanded molecular phylogeny that includes many of the species for which we have access to data on midband anatomy, filter numbers and filter spectral absorbance. We paid particular attention to species that are unusual compared with other stomatopods (for instance, the Pseudosquillidae, which have six-row midbands containing four filter classes, with some unique filter types seen in no other stomatopods but which are notably primitive in many other morphological features), and whenever possible we augmented our physiological database of filter spectral properties with new data from these and other species. We then used this new phylogeny, together with all available new and pre-existing data on ocular morphology and spectral characterizations of filters, to examine the evolution of a number of interesting visual physiological features of the stomatopods. Using ancestral state reconstructions, a phylogenetic method where character states at ancestral nodes of a phylogeny are inferred from the distribution of traits observed in extant species, we investigated the form and function of the ancestral stomatopod eye, and how it evolved

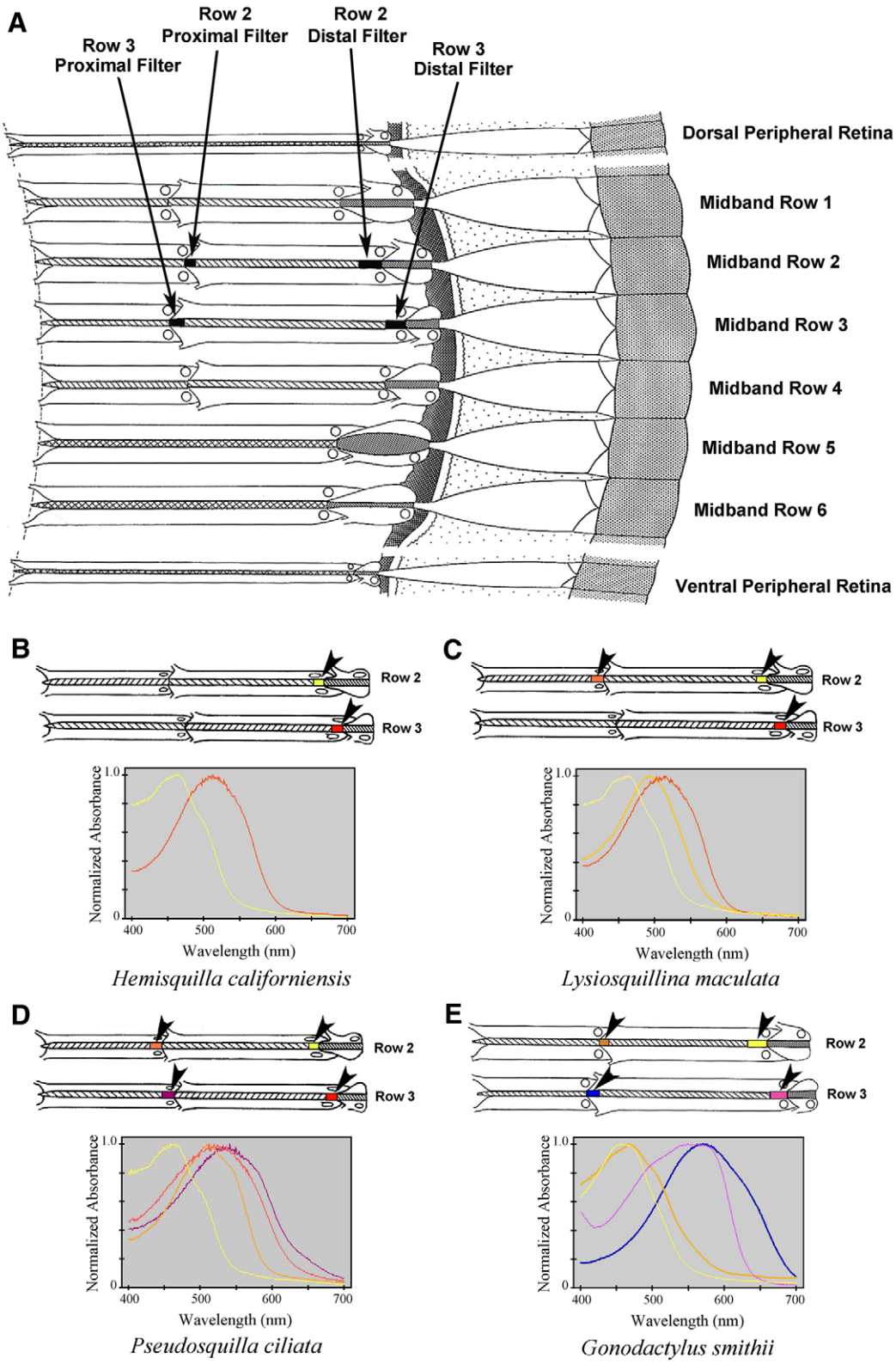


Fig. 2. (A) A diagrammatic view in vertical section of a typical stomatopod eye with a six-row midband, showing the numbering of the rows, retinal tiers in midband rows 1–4, and filter locations in rows 2 and 3. (B–E) Filter organization shown diagrammatically in midband rows 2 and 3 in various species (top part of each panel), together with absorbance spectra of filters (bottom part of each panel). Filter locations are indicated by arrowheads. Colors of filters in the diagrams and in the absorbance plots approximate their appearance in life. The species selected for illustration are: (B) *Hemisquilla californiensis*, with only two distal filter types; (C) *Lysiosquillina maculata*, which has two distal types and one proximal type, located in the row 2 proximal tier; (D) *Pseudosquilla ciliata*, with all four filter classes, with the row 2 proximal filter occurring in the proximal tier of the rhabdom; and (E) *Gonodactylus smithii*, which has all four filter types but with the row 2 proximal filter appearing in the distal tier of the rhabdom.

to form the complexity we observe today. Our results revealed the evolution and elaboration of advanced physiological features in a visually highly competent group of animals. By permitting a comparison of closely related species that inhabit diverse environments, this work also provides a unique view of how sensory systems adapt to complex or variable environments.

## MATERIALS AND METHODS

### Taxon sampling

Forty-nine species representing 11 families and four superfamilies were included in this study (Table 1). Most species chosen represent those where filter absorbance data were available or could be obtained. Those included in the phylogeny without filter data were

Table 1. Taxonomy and GenBank accession numbers for gene sequences from Stomatopoda included in this study

| Taxon | ID | 16S | COI | 18S | 28S-1 | 28S-2 |
|---|---|---|---|---|---|---|
| Gonodactyloidea | | | | | | |
| Gonodactylidae | | | | | | |
| *Gonodactylus childi* Manning 1971 | Gl | HM138825 | HM138784 | HM138869 | HM180013 | HM180057 |
| *Gonodactylus chiragra* (Fabricius 1781) | Gr | HM138826 | HM138785 | HM138870 | HM180014 | HM180058 |
| *Gonodactylus smithii* Pocock 1893 | Gs | HM138829 | HM138788 | HM138873 | HM180017 | HM180061 |
| *Gonodactylus platysoma* Wood-Mason 1895 | Gp | HM138828 | HM138787 | HM138872 | HM180016 | HM180060 |
| *Gonodactylaceus falcatus* (Forskål 1775) | Gf | HM138827 | HM138786 | HM138871 | HM180015 | HM180059 |
| *Gonodactylaceus graphurus* (Miers 1884) | Gg | **AF133678** | **AF048822** | NA | **FJ871157 / FJ871149** | NA |
| *Gonodactylellus affinis* (de Man 1902) | Gi | HM138823 | **AF205228** | HM138867 | HM180011 | HM180055 |
| *Gonodactylellus annularis* Erdmann and Manning 1998 | Gn | HM138824 | HM138783 | HM138868 | HM180012 | HM180056 |
| *Gonodactylellus espinosus* (Borradaile 1898) | Ge | HM138822 | HM138782 | HM138866 | HM180010 | HM180054 |
| *Neogonodactylus bahiahondensis* (Schmitt 1940) | Na | HM138836 | HM138794 | HM138880 | HM180024 | HM180068 |
| *Neogonodactylus bredini* (Manning 1969) | Nb | HM138837 | HM138795 | HM138881 | HM180025 | HM180069 |
| *Neogonodactylus oerstedii* (Hansen 1895) | No | HM138838 | HM138796 | HM138882 | HM180026 | HM180070 |
| Odontodactylidae | | | | | | |
| *Odontodactylus cultrifer* (White 1850) | Oc | HM138839 | NA | HM138883 | HM180027 | HM180071 |
| *Odontodactylus havanensis* (Bigelow 1893) | Oh | HM138840 | NA | HM138884 | HM180028 | HM180072 |
| *Odontodactylus latirostris* Borradaile 1907 | Ol | HM138841 | HM138797 | HM138885 | HM180029 | HM180073 |
| *Odontodactylus scyllarus* (Linnaeus 1758) | Os | HM138842 | HM138798 | HM138886 | HM180030 | HM180074 |
| Protosquillidae | | | | | | |
| *Chorisquilla excavata* (Miers 1880) | Ce | HM138816 | HM138776 | HM138860 | HM180004 | HM180048 |
| *Chorisquilla hystrix* (Nobili 1899) | Ch | HM138817 | HM138777 | HM138861 | HM180005 | HM180049 |
| *Chorisquilla tweedei* (Serène 1952) | Ct | HM138818 | HM138778 | HM138862 | HM180006 | HM180050 |
| *Echinosquilla guerinii* (White 1861) | Eg | HM138820 | HM138780 | HM138864 | HM180008 | HM180052 |
| *Haptosquilla glyptocercus* (Wood-Mason 1875) | Hg | HM138830 | HM138789 | HM138874 | HM180018 | HM180062 |
| *Haptosquilla trispinosa* (Dana 1852) | Ht | HM138831 | HM138790 | HM138875 | HM180019 | HM180063 |
| *Protosquilla folini* (A. Milne-Edwards 1867) | Pf | HM138843 | HM138799 | HM138887 | HM180031 | HM180075 |
| Takuidae | | | | | | |
| *Taku spinosocarinatus* (Fukuda, 1909) | Ts | HM138855 | HM138811 | HM138899 | HM180043 | HM180087 |
| Hemisquilloidea | | | | | | |
| Hemisquillidae | | | | | | |
| *Hemisquilla australiensis* Stephenson 1967 | Ha | **FJ871141** | NA | NA | **FJ871156 / FJ871148** | NA |
| *Hemisquilla californiensis* Stephenson 1967 | Hc | HM138832 | HM138791 | HM138876 | HM180020 | HM180064 |
| Lysiosquilloidea | | | | | | |
| Lysiosquillidae | | | | | | |
| *Lysiosquillina maculata* (Fabricius 1793) | Lm | HM138834 | HM138793 | HM138878 | HM180022 | HM180066 |
| *Lysiosquillina sulcata* Manning 1978 | Ls | HM138835 | NA | HM138879 | HM180023 | HM180067 |
| Nannosquillidae | | | | | | |
| *Alachosquilla vicina* (Nobili 1904) | Av | HM138812 | NA | HM138856 | HM180000 | HM180044 |
| *Austrosquilla tsangi* Ahyong 2001 | At | **FJ871139** | NA | NA | **FJ871145 / FJ871153** | NA |
| *Coronis scolopendra* Latreille 1828 | Cs | HM138819 | HM138779 | HM138863 | HM180007 | HM180051 |
| *Pullosquilla thomassini* Manning 1978 | Pt | HM138847 | HM138803 | HM138891 | HM180035 | HM180079 |
| Tetrasqullidae | | | | | | |
| *Heterosquilla tricarinata* (Claus 1871) | Hr | **FJ871140** | **AF048823** | NA | **FJ871146 / FJ871154** | NA |
| Parasquilloidea | | | | | | |
| Parasquillidae | | | | | | |
| *Pseudosquillopsis marmorata* (Lockington 1877) | Pm | HM138845 | HM138801 | HM138889 | HM180033 | HM180077 |
| Pseudosquilloidea | | | | | | |
| Pseudosquillidae | | | | | | |
| *Pseudosquilla ciliata* (Fabricius 1787) | Pc | HM138844 | HM138800 | HM138888 | HM180032 | HM180076 |
| *Pseudosquilliana richeri* (Moosa 1991) | Pr | HM138846 | HM138802 | HM138890 | HM180034 | HM180078 |
| *Raoulserenea hieroglyphica* (Manning 1972) | Rh | HM138848 | HM138805 | HM138892 | HM180037 | HM180081 |
| *Raoulserenea komaii* (Moosa 1991) | Rk | HM138849 | HM138804 | HM138893 | HM180036 | HM180080 |
| *Raoulserenea ornata* (Miers 1880) | Ro | HM138850 | HM138806 | HM138894 | HM180038 | HM180082 |
| *Raoulserenea oxyrhyncha* (Borradaile 1898) | Rx | HM138851 | HM138807 | HM138895 | HM180039 | HM180083 |
| *Raoulserenea n.* sp. | Rp | HM138852 | HM138808 | HM138896 | HM180040 | HM180084 |
| Squilloidea | | | | | | |
| Squillidae | | | | | | |
| *Alima orientalis* Manning 1978 | Ao | HM138813 | HM138773 | HM138857 | HM180001 | HM180045 |
| *Alima pacifica* Ahyong, 2001 | Ap | HM138814 | HM138774 | HM138858 | HM180002 | HM180046 |
| *Busquilla plantei* Manning 1978 | Bp | HM138815 | HM138775 | HM138859 | HM180003 | HM180047 |
| *Fallosquilla fallax* (Bouvier 1914) | Ff | HM138821 | HM138781 | HM138865 | HM180009 | HM180053 |
| *Harpiosquilla harpax* (de Haan 1844) | Hh | **FJ871137** | **FJ229770** | NA | **FJ871143 / FJ871151** | NA |
| *Kempina mikado* (Kemp and Chopra 1921) | Km | HM138833 | HM138792 | HM138877 | HM180021 | HM180065 |
| *Squilla empusa* Say 1818 | Se | HM138853 | HM138809 | HM138897 | HM180041 | HM180085 |
| *Squilla rugosa* Bigelow 1893 | Sr | HM138854 | HM138810 | HM138898 | HM180042 | HM180086 |
| Outgroups | | | | | | |
| *Anaspides tasmaniae* | At | **AF133694** | **DQ889076** | **L81948** | **AY859549** | NA |
| *Homarus americanus* | Ha | **AF370876** | **AF370853** | **AY743945** | **DQ079788** | NA |
| *Meganyctiphanes norvegica* | Mn | **AY744910** | **AF177191** | **DQ900731** | **AY744900** | NA |
| *Neomysis americana* | Na | HM179997 | **FJ581789** | HM179998 | HM179999 | NA |
| *Paranebalia longipes* | Pl | **AY744909** | NA | **EF189630** | **EF189655** | NA |

Underlined superfamily names are those proposed in this paper. Accession numbers in bold are sequences that were acquired from GenBank, and missing sequences are indicated by NA. The 28S-1 region spans expansion segments D2–D7b, while the 28S-2 region spans D9–D10 (Gillespie et al., 2006).

important for taxon sampling and stabilizing relationships among groups. Tissue samples were taken from each of the 44 species and stored in ethanol for use in generating the molecular data (e.g. nucleotide sequences from four phylogenetically informative genes; see below). Additionally, we included sequence data available from public databases for an additional five species (*Gonodactylaceus graphurus*, *Hemisquilla australiensis*, *Austrosquilla tsangi*, *Heterosquilla tricarinata* and *Harpiosquilla harpax*). Representatives of each species for which new sequences were generated were collected mainly from habitats surrounding one of the following locations: Lizard Island, Queensland, Australia; Moorea Island, French Polynesia; Beaufort, NC, USA; Key Largo, FL, USA; Oahu, HI, USA.

### DNA extraction, PCR and sequencing

Total genomic DNA was extracted from the muscle tissue of each species using a DNeasy Kit (Qiagen, Valencia, CA, USA). Polymerase chain reaction (PCR) products for the complete 18S rDNA (~2000 bp) and partial 28S rDNA (expansion segments D2–D7b and D9–D10, ~2800 bp) nuclear genes, and partial 16S (~460 bp) and cytochrome oxidase I (COI, ~650 bp) mitochondrial genes were amplified using one or more sets of general primers (Table 2). Standard PCR conditions (final concentrations in 25 µl: 1× buffer, 200 nmol $l^{-1}$ of each primer, 200 µmol $l^{-1}$ dNTPs and 1 U HotMaster taq from Eppendorf, Hauppauge, NY, USA) were used on a BioRad DNA Engine Thermal Cycler (Hercules, CA, USA) with the following cycling parameters: initial denaturation at 96°C for 2 min, followed by 40 cycles of 96°C for 1 min, 46°C for 1 min and 72°C for 1 min, followed by a final chain extension at 72°C for 10 min. PCR products were visualized by agarose gel electrophoresis and purified using the NucleoSpin Extract II kit (Machery Nagel, Bethlehem, PA, USA). Sequences were generated in both directions on an ABI PRISM 3100 Automated Capillary Genetic Analyzer (Applied Biosystems, Foster City, CA, USA) using the ABI Big-dye Ready-Reaction kit using 1/16th of the suggested reaction volume.

Table 2. The primer pairs used to amplify gene sequences used in the present study

| Amplified gene | Primer | Sequence (from 5′ to 3′) |
|---|---|---|
| 18S rDNA | 18S 1f | TAC CTG GTT GAT CCT GCC AGT AG |
| | 18S b5.0 | TAA CCG CAA CAA CTT TAA T |
| | 18S a0.7 | ATT AAA GTT GTT GCG GTT |
| | 18S bi | GAG TCT CGT TCG TTA TCG GA |
| | 18S ai | CCT GAG AAA CGG CTA CCA CAT C |
| | 18S b2.9 | TAT CTG ATC GCC TTC GAA CCT CT |
| | 18S a2.0 | ATG GTT GCA AAG CTG AAA C |
| | 18S 9R | GAT CCT TCC GCA GGT TCA CCT AC |
| COI | LCOI-1490 | GGT CAA CAA ATC ATA AAG ATA TTG |
| | HCOI-2198 | TAA ACT TCA GGG TGA CCA AAA AAT CA |
| 28S rDNA | 28S rD1a | CCC SCG TAA YTT AAG CAT AT |
| | 28S rD4b | CCT TGG TCC GTG TTT CAA GAC |
| | 28S A | GAC CCG TCT TGA AGC ACG |
| | 28S rD5b | CCA CAG CGC CAG TTC TGC TTA C |
| | 28S rD4.5a | AAG TTT CCC TCA GGA TAG CTG |
| | 28S rD7b1 | GAC TTC CCT TAC CTA CAT |
| | 28S 1F | GAG CCC AGC GCG GAA CCT CGC GC |
| | 28S 1R | CGC CTT TGG GTT TAG TGC GCC |
| | 28S 2F | AAT CTG GAG TAC CTA GTG GGC C |
| | 28S 2R | GAT CGC GGT ACT CAG GAC GCC G |
| | 28S 4F | CCT GTT GAG CTT GAC TCT AGT C |
| | 28S 4R | GTA GGG TAA AAC TAA CCT GTC |

18S and 28S rDNA primers are from Whiting et al. and Whiting (Whiting et al., 1997; Whiting, 2002) or were designed specifically for this study of stomatopods (28S 1F, 1R, 2F, 2R, 4F and 4R); 16S primers are from Crandall and Fitzpatrick, Jr (Crandall and Fitzpatrick, Jr, 1996); COI primers are from Folmer et al. (Folmer et al., 1994).

### Phylogenetic analyses

The most recent and extensive molecular study of arthropod phylogenetic relationships placed the Stomatopoda within the crustacean group Malacostraca (Regier et al., 2010). Therefore, to root the tree, representative sequences from all of the major lineages within the Malacostraca were used as outgroups (Table 1). Nucleotide sequences of the 16S, 18S and 28S genes were aligned with the online MAFFT server using the E-INS-I strategy (http://mafft.cbrc.jp/alignment/server/) (Katoh et al., 2002; Katoh et al., 2005). The COI sequences were inspected for evidence of pseudogenes (e.g. stop codons, indels not contiguous with codons) and then manually aligned using the translated amino acid sequences. Phylogenetic analyses of combined datasets can reveal hidden support for relationships in conflict among analyses of individual markers (Gatesy et al., 1999); therefore, the four gene regions were concatenated, and highly divergent and/or ambiguous regions of the entire alignment were removed using the program GBlocks (Castresana, 2000) using the following parameters: minimum number of sequences for a conserved position=28, minimum number of sequences for a flanking position=28, minimum number of contiguous non-conserved positions=10, minimum length of a block=2, allowed gaps=all. The combined dataset was used to reconstruct a phylogeny using maximum likelihood (ML) heuristic searches in PHYML (Guindon and Gascuel, 2003). Model selection was determined using jModelTest (Posada, 2008). ML searches were run using the general time reversible model (GTR), estimating the nucleotide frequencies and proportion of invariable sites. Confidence in the resulting relationships was assessed using approximate likelihood ratio tests (aLRTs) (Anisimova and Gascuel, 2006).

### Microspectrophotometry, filter classification and ancestral state reconstruction

To study the evolution of complexity in the stomatopod visual system, ancestral character states were reconstructed for the midband ommatidial row number, number of filter types and the filter spectral classes found at each intrarhabdomal filter location (Table 3). The methods of measuring spectral absorbance of the intrarhabdomal filters in stomatopod eyes have been described elsewhere (Cronin et al., 1994b). Briefly, eyes were removed, flash frozen and sectioned in a cryostat (8–14 µm thick). Sections containing filters were mounted in mineral oil between coverslips, and microspectrophotometry was performed using a single-beam instrument that obtains spectral data at 1 nm intervals from 400 to 700 nm (Cronin, 1985; Cronin and Marshall, 1989a). Absorbance values were computed by comparing the amount of light passing through the filter at each wavelength with the amount of light measured when the beam was placed in a clear area of the preparation. For each intrarhabdomal position, the highest quality scans from all study species at each homologous retinal location were exhaustively compared, side-by-side, to determine the distinct classes of filters based on the shape of the absorbance curve and spectral location. This resulted in identifying 2–7 classes of filters for each anatomical location, which have been named based on the row number (2 or 3), retinal position (D – distal, P – proximal) and

Table 3. The number of midband rows, the number of filters and the distribution of filter classes at each intrarhabdomal location for the species used for phylogenetic analyses and ancestral state reconstructions

| | R2D | R2P | R3D | R3P | #F | #MBR |
|---|---|---|---|---|---|---|
| Gonodactyloidea | | | | | | |
| Gonodactylidae | | | | | | |
| *Gonodactylus childi* | 2 | 4 | 3 | 3 | 4 | 6 |
| *Gonodactylus chiragra* | 2 | 7 | 3 | 3 | 4 | 6 |
| *Gonodactylus smithii* | 2 | 4 | 3 | 3 | 4 | 6 |
| *Gonodactylus platysoma* | 2 | 4 | 3 | 3 | 4 | 6 |
| *Gonodactylaceus falcatus* | 2 | 4 | 3 | 3 | 4 | 6 |
| *Gonodactylaceus graphurus* | ? | ? | ? | ? | ? | 6 |
| *Gonodactylellus affinis* | 2 | 4 | 2 | 2 | 4 | 6 |
| *Gonodactylellus annularis* | ? | ? | ? | ? | ? | 6 |
| *Gonodactylellus espinosus* | 2 | 4 | 2 | 3 | 4 | 6 |
| *Neogonodactylus bahiahondensis* | ? | ? | ? | ? | ? | 6 |
| *Neogonodactylus bredini* | 2 | 4 | 3 | 3 | 4 | 6 |
| *Neogonodactylus oerstedii* | 2 | 4 | 3 | 3 | 4 | 6 |
| Odontodactylidae | | | | | | |
| *Odontodactylus cultrifer* | ? | ? | ? | ? | ? | 6 |
| *Odontodactylus havanensis* | 1 | 3 | 1 | 1 | 4 | 6 |
| *Odontodactylus latirostris* | 1 | 3 | 1 | 1 | 4 | 6 |
| *Odontodactylus scyllarus* | 1 | 1 | 1 | 1 | 4 | 6 |
| Protosquillidae | | | | | | |
| *Chorisquilla excavata* | 2 | 2 | 1 | 1 | 4 | 6 |
| *Chorisquilla hystrix* | 2 | 3 | 2 | 3 | 4 | 6 |
| *Chorisquilla tweedei* | 2 | 4 | 3 | 3 | 4 | 6 |
| *Echinosquilla guerinii* | 2 | 2 | 1 | 1 | 4 | 6 |
| *Haptosquilla glyptocercus* | 2 | 4 | 3 | 3 | 4 | 6 |
| *Haptosquilla trispinosa* | 2 | 4 | 3 | 3 | 4 | 6 |
| *Protosquilla folini* | ? | ? | ? | ? | ? | 6 |
| Takuidae | | | | | | |
| *Taku spinosocarinatus* | 2 | 4 | 3 | 3 | 4 | 6 |
| Hemisquilloidea | | | | | | |
| Hemisquillidae | | | | | | |
| *Hemisquilla australiensis* | ? | ? | ? | ? | ? | 6 |
| *Hemisquilla californiensis* | 1 | 0 | 1 | 0 | 2 | 6 |
| Lysiosquilloidea | | | | | | |
| Lysiosquillidae | | | | | | |
| *Lysiosquillina maculata* | 1 | 5 | 1 | 0 | 3 | 6 |
| *Lysiosquillina sulcata* | 1 | 0 | 1 | 0 | 2 | 6 |
| Nannosquillidae | | | | | | |
| *Alachosquilla vicina* | 1 | 5 | 1 | 0 | 3 | 6 |
| *Austrosquilla tsangi* | 0 | 0 | 0 | 0 | 0 | 2 |
| *Coronis scolopendra* | 1 | 3 | 1 | 0 | 3 | 6 |
| *Pullosquilla thomassini* | 1 | 5 | 1 | 0 | 3 | 6 |
| Tetrasqullidae | | | | | | |
| *Heterosquilla tricarinata* | ? | ? | ? | ? | ? | 6 |
| Parasquilloidea | | | | | | |
| Parasquillidae | | | | | | |
| *Pseudosquillopsis marmorata* | ? | ? | ? | ? | ? | 3 |
| Pseudosquilloidea | | | | | | |
| Pseudosquillidae | | | | | | |
| *Pseudosquilla ciliata* | 1 | 6 | 2 | 2 | 4 | 6 |
| *Pseudosquilliana richeri* | ? | ? | ? | ? | ? | 6 |
| *Roulserenea hieroglyphica* | 1 | 6 | 2 | 2 | 4 | 6 |
| *Roulserenea komaii* | ? | ? | ? | ? | ? | 6 |
| *Roulserenea ornata* | ? | ? | ? | ? | ? | 6 |
| *Roulserenea oxyrhyncha* | ? | ? | ? | ? | ? | 6 |
| *Roulserenea n.* sp. | 1 | 6 | 2 | 2 | 4 | 6 |
| Squilloidea | | | | | | |
| Squillidae | | | | | | |
| *Alima orientalis* | 0 | 0 | 0 | 0 | 0 | 2 |
| *Alima pacifica* | 0 | 0 | 0 | 0 | 0 | 2 |
| *Busquilla platei* | 0 | 0 | 0 | 0 | 0 | 2 |
| *Fallosquilla fallax* | 0 | 0 | 0 | 0 | 0 | 2 |
| *Harpiosquilla harpax* | 0 | 0 | 0 | 0 | 0 | 2 |
| *Kempina mikado* | 0 | 0 | 0 | 0 | 0 | 2 |
| *Squilla empusa* | 0 | 0 | 0 | 0 | 0 | 2 |
| *Squilla rugosa* | 0 | 0 | 0 | 0 | 0 | 2 |
| Outgroups | | | | | | |
| *Anaspides tasmaniae* | 0 | 0 | 0 | 0 | 0 | 0 |
| *Homarus americanus* | 0 | 0 | 0 | 0 | 0 | 0 |
| *Meganyctiphanes norvegica* | 0 | 0 | 0 | 0 | 0 | 0 |
| *Neomysis americana* | 0 | 0 | 0 | 0 | 0 | 0 |
| *Paranebalia longipes* | 0 | 0 | 0 | 0 | 0 | 0 |

R2D=row 2 distal filter location, R2P=row 2 proximal filter location, R3D=row 3 distal filter location, R3P=row 3 proximal filter location, #F=number of intrarhabdomal filters, #MBR=number of midband rows, and ?=missing data. Underlined superfamily names are those proposed in this paper.

a unique class number (e.g. 2D-1; see Table 3). It is important to note that in the original data, no spectrum from a set placed in any of these classes ever replicated that of a different class.

For reconstructing the number of midband rows, number of filters and filter class ancestral character states, the PHYML tree was imported into the program Mesquite v2.72 (Maddison and Maddison, 2009). Species without data on filter number and spectral classes were pruned from the tree before reconstruction. All characters (e.g. number of midband rows, number of filters, spectral classes found at each filter location) were assigned as standard categorical characters. In order to avoid reconstructing non-homologous characters (e.g. the presence and absence of a character *versus* the state of a character when present), in species where filters are absent, the filter characters (e.g. filter number and spectral class at each intrarhabdomal location) were coded as missing data. Ancestral states for each character were inferred under the MK1 ML model and reconstructions were mapped onto the phylogeny.

## RESULTS

### Stomatopod phylogenetics

We obtained 39 new COI and 44 new 18S, 28S and 16S gene sequences (Table 1). With data available from GenBank, we constructed the most comprehensive molecular phylogeny of

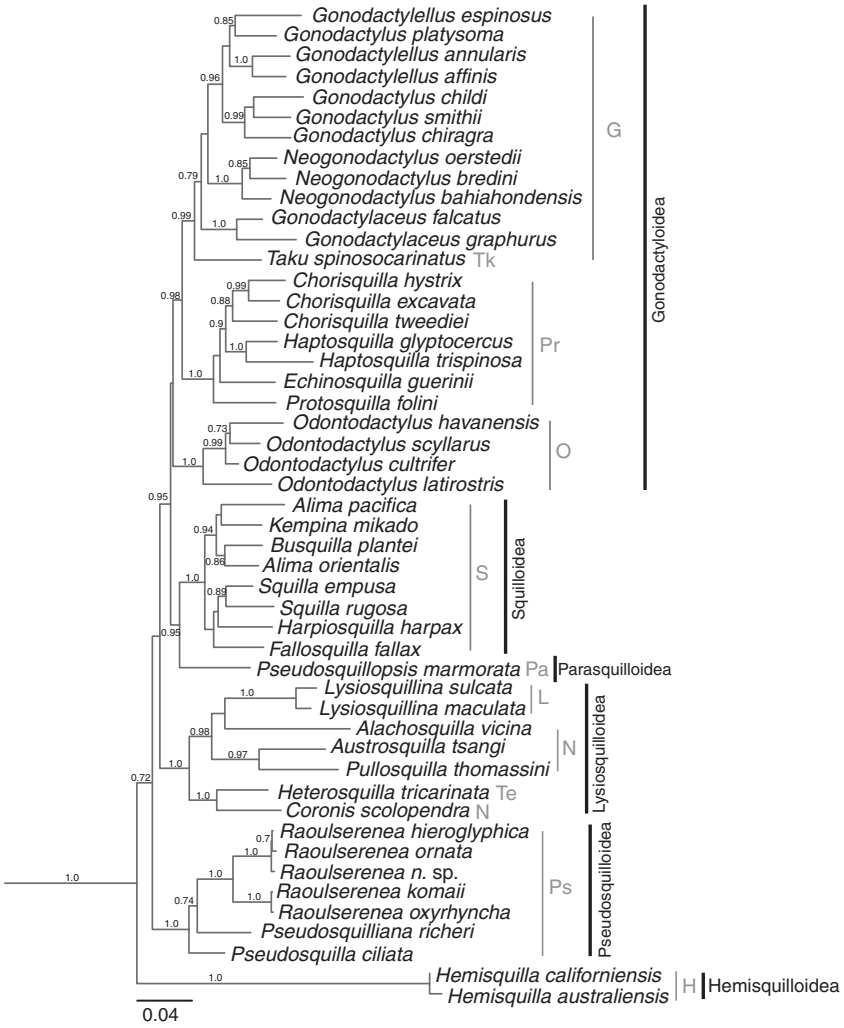


Fig. 3. Maximum likelihood phylogeny of stomatopod relationships, reconstructed using PHYML, with the outgroups not shown due to long branch lengths. Branch support values represent approximate likelihood ratio tests. Light gray letters indicate families as follows: G – Gonodactylidae; H – Hemisquillidae; L – Lysiosquillidae; N – Nannosquillidae; O – Odontodactylidae; Pa – Parasquillidae; Pr – Protosquillidae; Ps – Pseudosquillidae; S – Squillidae; Te – Tetrasquillidae; Tk – Takuidae.

stomatopod species to date, including 49 species. In our phylogeny, most of the families represented, and most of the genera with more than one representative species, were recovered as monophyletic clades with strong nodal support (aLRT=0.98–1.0, Fig. 3). Exceptions include the clustering of *Gonodactylus platysoma* with the remaining *Gonodactylellus* species and the polyphyly of the two included *Alima* species and of the species within the Nannosquillidae. There is also strong support for the superfamilies Squilloidea (aLRT=1.0) and Lysiosquilloidea (aLRT=1.0), and for a sister relationship between the Squilloidea, containing two midband rows, and the Parasquilloidea, containing three midband rows (aLRT=0.95). The recovered relationships within the Gonodactyloidea, however, are not congruent with current stomatopod taxonomy. The families within the superfamily Gonodactyloidea are polyphyletic, with the Hemisquillidae and Pseudosquillidae forming lineages that are basal to all of the remaining stomatopods. There is also strong support for a relationship between the Gonodactyloidea (excluding the Hemisquillidae and Pseudosquillidae) and the Squilloidea and Parasquilloidea (aLRT=0.95). Although the placements of the Lysiosquilloidea and the Pseudosquillidae relative to each other are not strongly supported in our phylogeny, nodal supports suggest that they are distinct from both the basal lineage Hemisquillidae and from the lineage containing the Squilloidea, Parasquilloidea and the remaining Gonodactyloidea.

### Visual character evolution

Morphologically, the most obviously unique features of the stomatopod eye are the midband rows and intrarhabdomal filters (Figs 1, 2). Character state reconstructions show that the most complex eye type, with six midband rows and four intrarhabdomal filters, was present in the ancestral stomatopod lineage (Figs 4, 5). Three of the stomatopod lineages included in our study then lose morphological complexity, with the hemisquillids losing the two proximal filter locations, the lysiosquilloids losing the row 3 proximal filter, and the squilloids and parasquilloids losing midbands rows and all filter sets (Figs 4, 5). The reduction of morphological complexity in these lineages is confirmed by the strong support for their phylogenetic position as nested within groups containing more complex eyes, particularly in Squilloidea and Parasquilloidea (aLRT=0.95).

The most spectrally simple intrarhabdomal filter is the midband row 2 distal filter. In this filter location, only two spectrally similar filter types have been found, differing consistently in the shape of the absorbance curve (Fig. 6). By contrast, the most diverse intrarhabdomal filter is the midband row 2 proximal filter, which has at least seven distinct filter classes (Fig. 7). Two classes of the row 2 proximal filter are identical to those found in the row 2 distal filter. The other five classes are spread over the spectrum, with peaks found from ~465 to 535 nm, and broadening absorbance curves as the peak wavelengths are red shifted. The midband row 3 distal and proximal intrarhabdomal filter locations both contain three types of

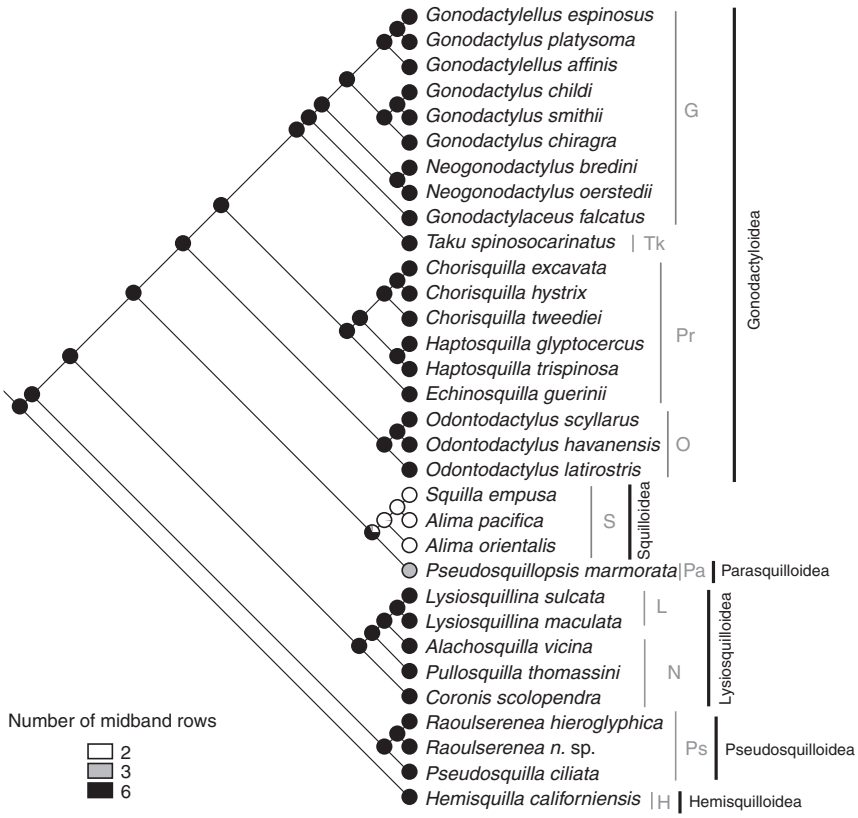


Fig. 4. Maximum likelihood ancestral state reconstruction of the number of midband rows using the stomatopod phylogeny from Fig. 3. At each node, a pie chart represents the proportional likelihood of each character state, with each state colored as in the key.

filters (Figs 8, 9). Over the course of stomatopod evolution, the filters in both of the row 3 locations have been shifted to absorb longer wavelengths of light, with the distal class 3 filter also exhibiting a broader absorbance curve (Fig. 8).

## DISCUSSION

### Stomatopod evolution

The stomatopods include many species with unique and complex visual systems, and several features of their eyes exist in no other animals. Although the physiology and visual function of stomatopod eyes have been studied for many years, how these unique visual features originated and diversified has been an open question. Understanding the evolutionary relationships among species is crucial for deciphering visual function in this group and can lead to insights into how color vision became specialized, as well as how eye function is associated with the occupation of particular visual environments. Until recently, most studies of relationships among stomatopod superfamilies have been based on morphological features, often including eye characters (Manning et al., 1984a; Ahyong, 1997; Ahyong and Harling, 2000). Harling, however, noted that eye characters are often misleading in deriving stomatopod relationships, particularly at higher levels (Harling, 2000). Thus, our first objective was to determine the most accurate possible picture of evolution and functional diversification of modern stomatopods. As we were particularly interested in visual evolution, we wanted to exclude characters related to vision from the analysis. For this and other reasons, we decided to use a strictly molecular approach to deriving a new stomatopod phylogeny.

Ahyong and Jarman recently published the first molecular study investigating stomatopod relationships among more than one superfamily, including 19 species (Ahyong and Jarman, 2009). Our study expands on the numbers of currently described species ($N$=49), families ($N$=10) and superfamilies ($N$=4) represented in molecular analyses and on the amount of sequence data used for phylogenetic analyses. Like Ahyong and Jarman (Ahyong and Jarman, 2009), we determined that the superfamilies Squilloidea and Lysiosquilloidea are each monophyletic (i.e. all species in each superfamily grouped on the same branch of the phylogeny) but that the Gonodactyloidea are polyphyletic, with subgroups formerly placed in this superfamily appearing in separate parts of the tree (Fig. 3). In particular, the placement of the families Hemisquillidae and Pseudosquillidae at the base of the tree, well outside of the regions containing the other gonodactyloid families, is significant from the perspective of visual system evolution, as both families have very different visual systems from the remaining members of the superfamily. Hemisquillids differ from the other gonodactyloids in having only two sets of intrarhabdomal filters present (Cronin et al., 1994a; Cronin et al., 1994b), while pseudosquillids have some unique types of filter classes as well as an unusual organization of receptors and filters in their midband eyes (for details, see below and Fig. 2) (Marshall et al., 1991a; Marshall et al., 1991b).

Because our phylogeny is congruent with Ahyong and Jarman's (Ahyong and Jarman, 2009) findings showing that the lineages Hemisquillidae and Pseudosquillidae are distinct from the remaining Gonodactyloidea, we provisionally elevate these groups to new superfamilies – the Pseudosquilloidea and the Hemisquilloidea. For the remainder of the discussion we will refer to these lineages using the provisional names, and will use 'Gonodactyloidea' to represent the group in Fig. 3 comprised of the families Gonodactylidae, Takuidae, Protosquillidae and Odontodactylidae.

Our phylogeny differs from that of Ahyong and Jarman (Ahyong and Jarman, 2009) in the relationships among the superfamilies. The 2009 analysis places the Squilloidea, containing two midband rows and no intrarhabdomal filters, as being most closely related to the Lysiosquilloidea, with six midband rows and two or three filters. By contrast, our analysis of stomatopod relationships

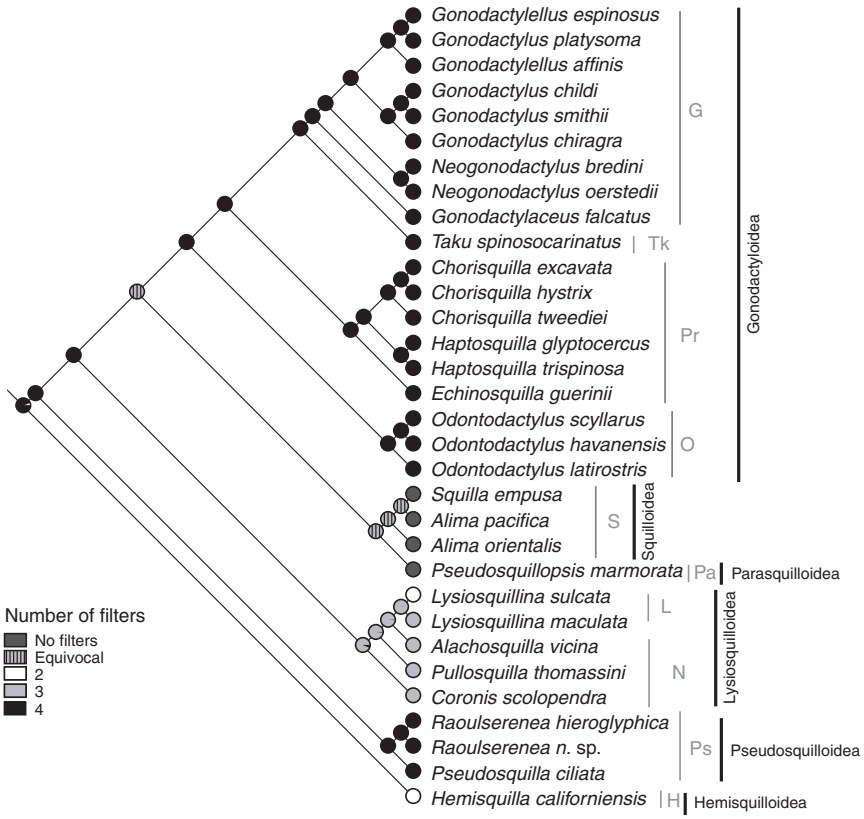


Fig. 5. Maximum likelihood ancestral state reconstruction of the number of intrarhabdomal filter locations within the retina using the stomatopod phylogeny from Fig. 3. At each node, a pie chart represents the proportional likelihood of each character state, with each state colored as in the key.

somewhat surprisingly places the Squilloidea (with the Parasquilloidea) as being most closely related to the Gonodactyloidea, having the most complex eyes with six midband rows and four filter types. In either case, the reduced numbers of midband rows and filters found in squilloids must represent evolutionary losses of complexity (see below for a more detailed discussion). The three superfamilies that have not yet been included in molecular phylogenies due to the difficulty in obtaining specimens – Bathysquilloidea, Erythrosquilloidea and Eurysquilloidea – demand future study to strengthen our understanding of stomatopod eye evolution.

### Evolution of stomatopod eyes

The design of the ancestral stomatopod eye has long been debated (Manning et al., 1984a; Manning et al., 1984b; Ahyong and Harling, 2000; Harling, 2000). To help resolve this controversy, we used our new phylogeny together with the physiological and anatomical characterization of stomatopod eyes to perform the first ancestral state reconstruction of stomatopod visual system characters, where character states at ancestral nodes of a phylogeny are inferred from the distribution of traits observed in extant species (Figs 4–9). Our analyses of midband row and intrarhabdomal filter numbers indicate that ancestral stomatopod eyes already contained the most complex type with six midband rows and all four types of filters (Figs 4, 5). Unfortunately, the relationships among the most basal lineages in the tree – the Hemisquilloidea, Lysiosquilloidea and Pseudosquilloidea – are not well supported, making reconstructions of the most basal nodes less reliable. Thus, we still cannot be certain how filters became added to stomatopod eyes; if the Lysiosquilloidea were more basal than the Pseudosquilloidea, then filter evolution may have progressed through a series of two filters (Hemisquilloidea), then two or three filters (Lysiosquilloidea) and finally four filters (Pseudosquilloidea and Gonodactyloidea). It is also interesting to note that the position of the row 2 proximal filter in the pseudosquilloids and lysiosquilloids is unlike that in the gonodactyloids. In gonodactyloid species, the row 2 proximal filter is formed from the distal photoreceptor cells but the filter at the same location in the Lysiosquilloidea and Pseudosquilloidea is formed by the proximal photoreceptor cells (see Fig. 2). This adds additional support to the conclusion that although the particular relationships between these two groups is still not strongly supported, with respect to filters, they are both distinct from all other stomatopod lineages.

Despite the potential uncertainty in the relationships at the base of the phylogeny, the ancestral lineage evidently already contained four filters, and filters have been lost independently at least three times: in the Hemisquilloidea, Lysiosquilloidea, and Squilloidea + Parasquilloidea. Invariably, in the groups that retain the six midband rows in their eyes (i.e. the Hemisquilloidea and Lysiosquilloidea), it is the proximal filters that are lost. Functionally, the serial filtering of midband rows 2 and 3 results in significantly reduced light intensities reaching the proximal photoreceptor (see Cronin et al., 1994c). Because of this sensory constraint, it is not surprising that the proximal filters are the first to be lost, particularly when species inhabit low-light, or spectrally limited, environments that may critically reduce the light available to the proximal photoreceptor.

As noted above, the superfamilies Squilloidea and Parasquilloidea contain eyes with both reduced numbers of midband rows and no intrarhabdomal filters. In squilloids, there are only two untiered midband rows, suggesting homology to midband rows 5 and 6 in six midband row eyes. Microspectrophotometry indicates that retinas of the squilloid *Squilla empusa* have but a single visual pigment (Cronin, 1985), but our recent investigations of visual pigment (opsin) expression in this species suggest that at least four different visual pigments are expressed in the retina (Porter et al., 2009; Cronin et al., 2010). The expression of multiple,

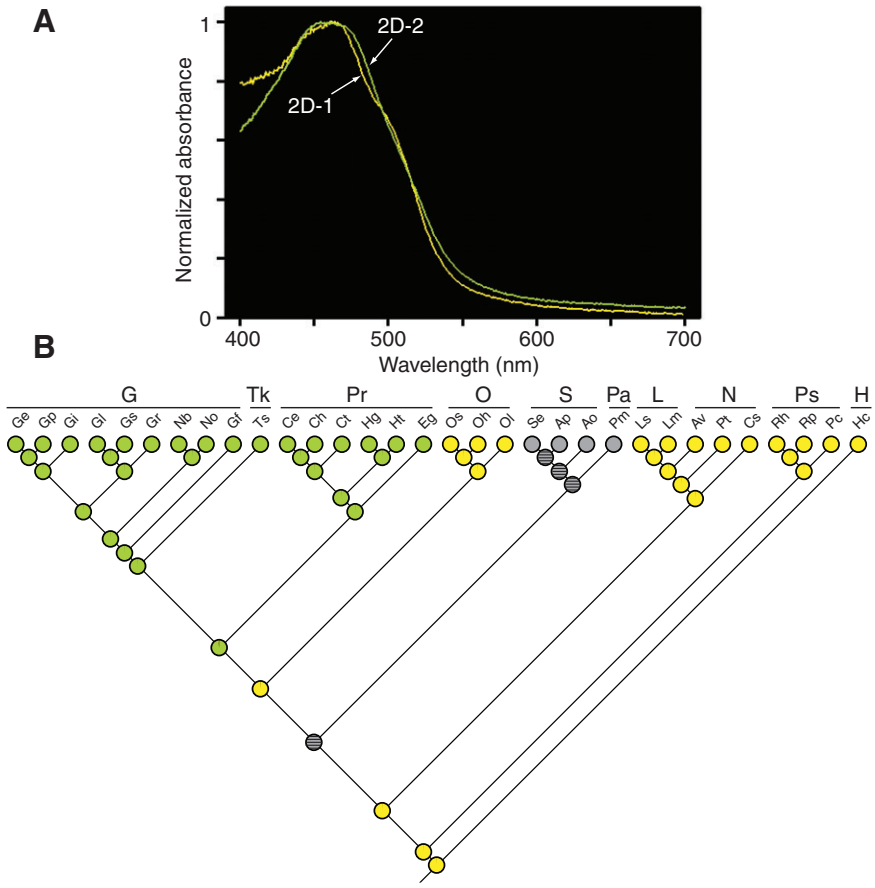


Fig. 6. Evolutionary reconstruction of the row 2 distal filter type. (A) Normalized absorbance spectra of single, high-quality scans representing each of the two spectral classes of filter found in the row 2 distal intrarhabdomal position. Both filter classes appear yellow in color in life but here class 2D-2 is colored green for clarity. The class 2D-1 spectrum is from *Hemisquilla californiensis*, while class 2D-2 is from *Gonodactylus smithii*. (B) Maximum likelihood ancestral state reconstruction of the filter classes onto the stomatopod phylogeny from Fig. 3, with species lacking data on filters removed from the tree. At each node, a pie chart represents the proportional likelihood of the presence of a particular filter class, with each filter class colored as in panel A. Solid gray circles represent species where this filter is not found, and gray and black striped circles represent nodes where the data for multiple classes are equivocal. Species are designated by the two-letter code found in Table 1. Families are indicated as follows: G – Gonodactylidae; H – Hemisquillidae; L – Lysiosquillidae; N – Nannosquillidae; O – Odontodactylidae; Pa – Parasquillidae; Pr – Protosquillidae; Ps – Pseudosquillidae; S – Squillidae; Tk – Takuidae.

phylogenetically distinct opsin genes in the *S. empusa* retina further supports the position of squilloids as derived from ancestors containing the most complex six midband eye type. Further study of opsin expression patterns in the retina of this species may help to elucidate the homology of the midband photoreceptors. The three midband rows in *Pseudosquillopsis marmorata* are also not tiered, making it difficult to determine homology relative to six midband row eyes. Why these two groups retain any functional midband photoreceptors at all remains an enigma; it is possible that the remaining midband rows serve as specialized polarized light detectors, as in rows 5 and 6 of the more complex eye designs, or that a midband is required in order to keep the peripheral receptors properly separated for spatial orientation and range finding.

Our findings support Harling (Harling, 2000), who previously suggested that the reduced morphologies observed in the eyes of several stomatopod groups must represent regressive loss, perhaps driven by shifts to either simpler, less colorful environments (Lysiosquilloidea), or dimmer habitats associated with either deeper, murkier waters or with nocturnal lifestyles (Hemisquilloidea, Squilloidea, Parasquilloidea). It is interesting to note that in the deep-living populations of some species, receptors in the third midband row degenerate, containing neither filters nor detectable visual pigments (Cronin et al., 1996; Cronin and Caldwell, 2002; Cronin et al., 2002). These particular receptors are sensitive to the longest wavelengths, which are rapidly attenuated by seawater and thus unavailable for vision at depth. This phenomenon implies that losing midband rows after shifts to darker habitats may be an evolutionarily easy task; if these rows become non-functional, selection to remove them could act rapidly to produce a simpler midband (analogous to the evolutionarily rapid, repeated losses of eyes in blind cavefish) (see Dowling et al., 2002). In the future, taxonomic placement of the unsampled stomatopod superfamilies (Bathysquilloidea and Erysquilloidea that lack midbands entirely; Eurysquilloidea with two or six midband rows) using molecular techniques will help to elucidate whether this loss of midband rows has happened convergently more than one time in stomatopods, as well as potentially providing essential information about the design of primitive stomatopod eyes.

### Evolution of spectral filtering

The extraordinary color vision system possessed by many stomatopod species would not be possible without the extensive use of spectral filtering. In the dorsal four midband rows, which underlie color vision in these animals (Marshall, 1988; Marshall et al., 1996), the main rhabdoms are divided into two photoreceptive tiers, formed from subsets of retinular cells 1–7 (Fig. 2) (Marshall, 1988; Marshall et al., 1991a; Marshall et al., 1991b). These tiered photoreceptors contain visual pigments with spectral maxima ranging from 400 nm to ~500 nm; the visual pigment of the distal tier invariably has a shorter wavelength absorption maximum than its mate in the proximal photoreceptive tier (Cronin and Marshall, 1989a; Cronin and Marshall, 1989b; Cronin et al., 1994a; Cronin and Marshall, 2004). With such an arrangement, the visual pigment in the top layer filters out shorter wavelengths before they reach the deeper layer, narrowing its spectral sensitivity and tuning it to longer wavelengths. In rows 1 and 4, which are devoted to short and middle wavelength sensitivity, the filtering action of the visual pigment alone is sufficient. Rows 2 and 3, however, have become further specialized to analyze long wavelength light, beyond about 550 nm. Visual pigments with maxima at longer wavelengths are

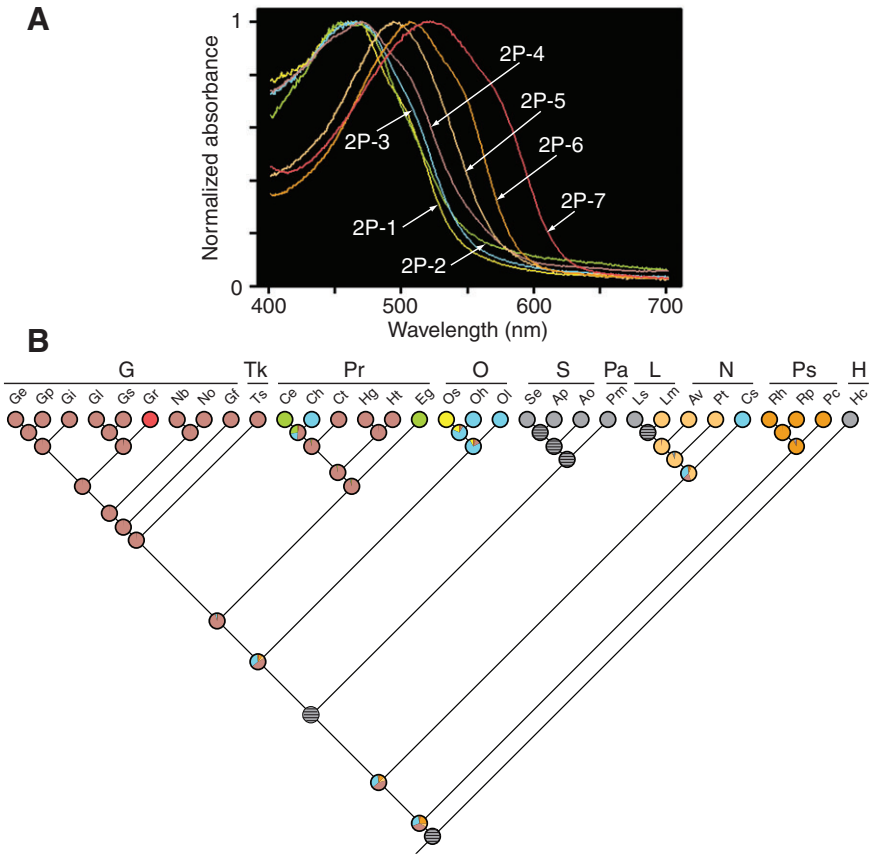


Fig. 7. Evolutionary reconstruction of the row 2 proximal filter type. (A) Normalized absorbance spectra of single, high-quality scans representing each of the seven spectral classes of filter found in the row 2 proximal intrarhabdomal position. In general, the colors of the various traces suggest the appearances of the filters in life but as classes 2P1–2P3 all appear yellow, class 2P-2 is colored green and class 2P-3 is cyan for clarity. The sources of the spectra are as follows: class 2P-1, *Odontodactylus syllarus*; class 2P-2, *Chorisquilla excavata*; class 2P-3, *Coronis scolopendra*; class 2P-4, *Gonodactylellus affinis*; class 2P-5, *Lysiosquillina maculata*; class 2P-6, *Raoulserenea hieroglyphica*; class 2P-7, *Gonodactylus chiragra*. (B) Maximum likelihood ancestral state reconstruction of the filter classes onto the stomatopod phylogeny from Fig. 3. Otherwise as in Fig. 6.

not used; instead, mantis shrimps use photostable filters for the required tuning. These are based on strongly colored pigments incorporated at the top of the main rhabdom (the distal filter) and commonly between its two photoreceptive tiers (the proximal filter). Thus, we now find species of mantis shrimps with six midband row eyes using two, three or four types of filters for spectral tuning (Fig. 2). While it seems reasonable that the numbers of spectral classes of pigments used within each of these anatomical filter locations increased as stomatopods evolved, until now it has not been possible to examine this hypothesis.

To investigate the evolution of spectral filtering in stomatopod visual systems, we first classified the filter types found at each intrarhabdomal location based on absorbance characteristics (Figs 6–9). Carrying out this classification required the visual inspection and direct spectral comparison of thousands of spectral scans from a total of 51 species of mantis shrimps (many of these species were unfortunately unavailable for the current genetic analysis), a far larger and higher quality dataset than was available for our 1994 study (Cronin et al., 1994b). Despite the availability of much new data, essentially the same filter classes as those assigned in the earlier paper were recovered. The classes of filters at the distal position in row 2 and at the proximal position in row 3 are identical to those of the 1994 paper (Cronin et al., 1994b). At the proximal position in row 2, two additional filter classes were found: one identical to class 1 of the row 2 distal position, and one new class very similar to class 2 of the distal position (Figs 6, 7). At the distal position of row 3, incorporation of new data actually reduced the number of classes from four to three. This filter type is unusually labile, even in a single preparation, sometimes changing in spectral shape between scans of the same material (Cronin et al., 1994b). Consequently, we removed one of the four classes assigned in 1994 because it represented a variation of another class (Fig. 8, 3D-2). As will be noted below, in fact, some stomatopod species have the ability to alter the filters present in the third midband row to other classes as they adapt to different photic environments.

Using these classes, we once more used phylogenetic reconstruction to investigate the ancestral filter states and to discover their functional diversification at each of the four filter locations. The simplest set of filter classes is found at the row 2 distal filters, which fall into two very similar classes, both absorbing maximally near 450–460 nm (Fig. 6). As noted in the last paragraph, the distal row 3 filters are not only more disparate in absorbance maxima but are also more variable and often less stable. In the lysiosquilloids, most of which have three filter types, the third filter is located in the row 2 proximal location. Across species, this is also the filter type containing the largest number of spectral classes (Fig. 7). The remaining filter location, row 3 proximal, is fairly conservative in the number of classes observed among species, containing only three (Fig. 9). However, like its mate in the row 3 distal position, this filter can vary within a species, sometimes even in a single retina (Cronin et al., 2001; Cronin and Caldwell, 2002; Cheroske et al., 2003; Cheroske et al., 2006).

Most families (and even superfamilies) included in our study are highly consistent in the filter class used at each location (Figs 6–9). However, the Gonodactyloidea are extremely variable in the filter classes used, with species containing all three filter classes found in the row 3 distal and proximal filters, and five of the seven classes found in the row 2 proximal filter. Additionally, a well-supported (aLRT=0.98) group of gonodactyloid families (e.g. the Gonodactylidae, Protosquillidae and Takuidae) includes all of the species that we have included in our study (or seen in

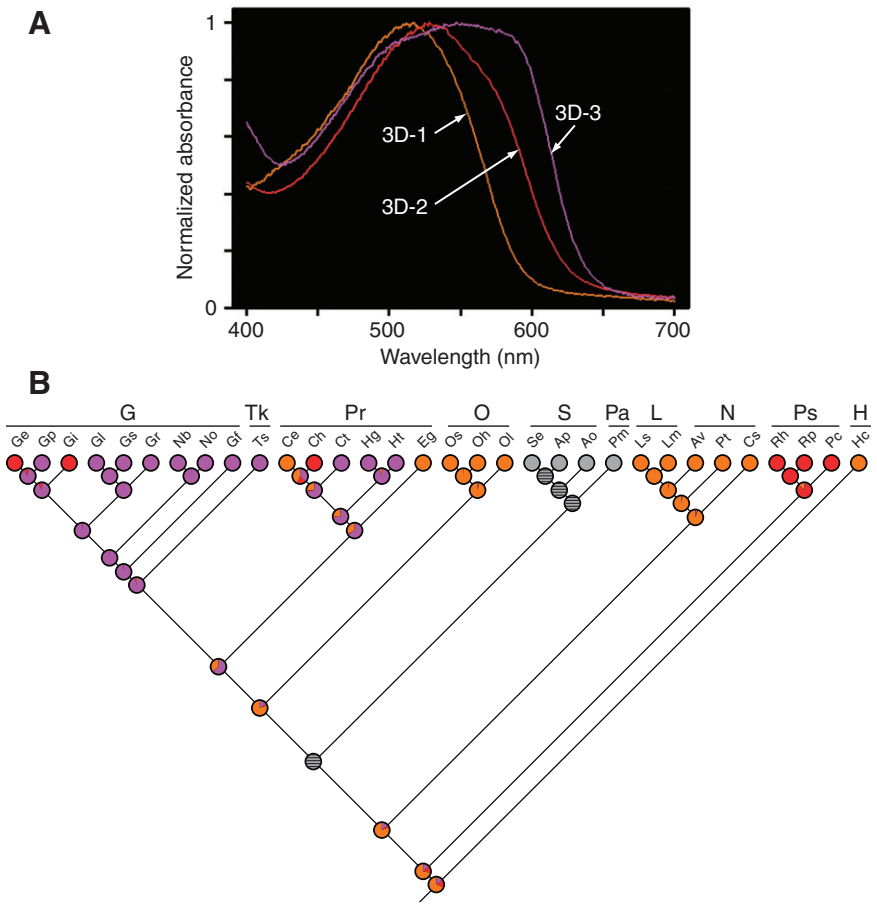


Fig. 8. Evolutionary reconstruction of the row 3 distal filter type. (A) Normalized absorbance spectra of single, high-quality scans representing each of the three spectral classes of filter found in the row 3 distal intrarhabdomal position. The colors of the traces reflect the appearance of the filter in life. Sources of spectra: class 3D-1, *Odontodactylus latirostris*; class 3D-2, *Gonodactylellus espinosus*; class 3D-3, *Gonodactylaceus falcatus*. (B) Maximum likelihood ancestral state reconstruction of the filter classes onto the stomatopod phylogeny from Fig. 3. Otherwise as in Fig. 6.

our more extensive examination of species that could not be analyzed phylogenetically) that use a different class of yellow filter in the row 2 distal position (Fig. 6). Although the advantage of switching filter types is unclear when the filter absorbance characteristics of both row 2 distal classes are so similar, all characterized members of these families use the unique 2D-2 filter.

During the evolution of spectral filtering in stomatopod visual systems, some species repeat filter types among different intrarhabdomal filter locations within the eye. For instance, the row 2 distal filter pigments of some species appear again in the row 2 proximal filters (e.g. *Odontodacylus scyllarus*, *Chorisquilla excavata* and *Echinosquilla guerinii*; Fig. 7). It is interesting to note that in these three species, the protosquillids (*C. excavata* and *E. guerinii*) revert to the pigment of the row 2 distal 2D-2 filters, while *O. scyllarus* uses the row 2 distal 2D-1 filter pigment; this presents intriguing evidence that this filter set is genetically determined, with the lineage including the Gonodactylidae, Takuidae and Protosquillidae having evolved a novel metabolic pathway or pigment assembly system. Similarly, the row 3 filter locations use some of the same filter pigments both distally and proximally, with the row 3 distal 3D-2 filters reappearing as the row 3 proximal 3P-1 filters (Figs 8, 9). Interestingly, a pigment with a very similar absorbance curve reappears in *Gonodactylus chiragra* in the row 2 proximal filter (the 2P-7 filter; Fig. 7). We consider some of the features producing the observed gonodactyloid filter diversity in the following paragraphs.

An intriguing aspect of adaptive tuning by stomatopods using spectral filters is that filters in row 2 and row 3 are employed quite differently. Note that while the distal filter locations display relatively conservative use of sets of filter classes, the proximal filter locations in these two rows use different mechanisms for fine tuning the visual system to the different light environments encountered by species that occur over a wide range of depths. In row 2, the proximal filter location contains by far the largest diversity of spectral classes, with each major lineage constructing a unique filter class and the majority of the diversity found within the Gonodactyloidea. However, the 2P-3 filter is found in *C. excavata* (Protosquillidae, Gonodactyloidea), several species of Odontodactylidae (Gonodactyloidea) and in *Coronis scolopendra* (Nannosquillidae, Lysiosquilloidea). The occurrence of this filter class in several distinct families suggests that either this particular filter pigment is easy to build and incorporate or our taxon sampling may be missing some of the variation among species in filters at this location.

Thus, the row 2 photoreceptors, particularly in the Gonodactyloidea, use spectral diversity in the proximal filter to tune the row for the environmental light available across the range of the species. The majority of the species in the Gonodactyloidea live in shallow, coral reef habitats, where near full-spectrum light is available and the surrounding environment is a riotous display of color. In this group, the row 2 proximal filter classes, which transmit at considerably shorter wavelengths relative to the homologous filters of lysiosquilloids or pseudosquilloids, adapt the color receptors to sample a spectrally broad and colorful photic environment (Figs 2, 7). A particularly spectacular case of the row 2 proximal filter tuning the underlying photoreceptor to the photic environment is the red-colored filter (Fig. 7; 2P-7) in *G. chiragra*. This species lives intertidally in the Great Barrier Reef in Australia, in some of the shallowest and most brightly lit water inhabited by

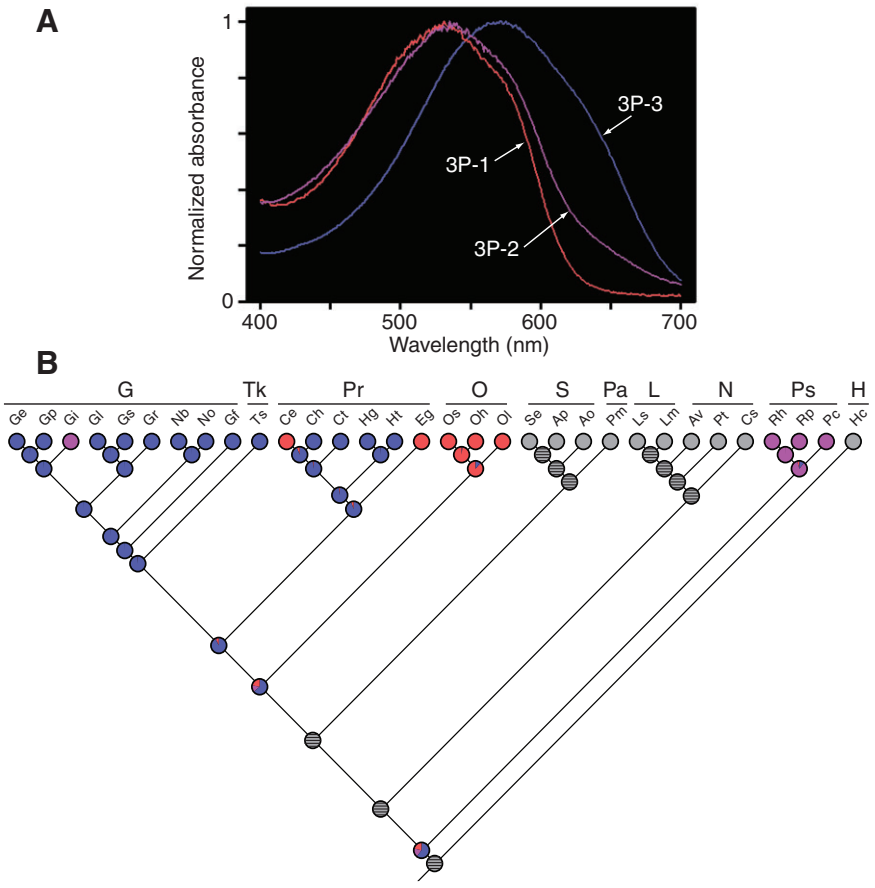


Fig. 9. Evolutionary reconstruction of the row 2 proximal filter type. (A) Normalized absorbance spectra of single, high-quality scans representing each of the three spectral classes of filter found in the row 3 proximal intrarhabdomal position; colors of the traces suggest the appearance of the filter in life. Sources of spectra: class 3P-1, *Odontodactylus scyllarus*; class 3P-2, *Raoulserenea n.* sp.; class 3P-3, *Gonodactylus smithii.* (B) Maximum likelihood ancestral state reconstruction of the filter classes onto the stomatopod phylogeny from Fig. 3. Otherwise as in Fig. 6.

any mantis shrimp, where its color vision system apparently profits from an extreme spectral range to sample the broad spectrum available from direct sunlight.

Unlike the invariant filters in row 2, in many mantis shrimp species the row 3 filters in both the distal and the proximal location are 'tunable' within an individual based on the available environmental light (Cronin et al., 2001; Cronin and Caldwell, 2002; Cheroske et al., 2003; Cheroske et al., 2006). Because of this flexibility, a large set of diverse filters is not required here to tune the underlying photoreceptors. While most of the yellow, orange and red pigments found in row 2 filters have spectra characteristic of carotenoid pigments, the row 3 proximal filters are instead thought to incorporate carotenoproteins (Cronin et al., 1994b). Color change in the row 3 proximal filter is apparently due to the interconversion of a carotenoprotein incorporating astaxanthin (possibly crustacyanin) between a complex, multimeric α-form creating a blue filter pigment, to a simpler (generally dimeric) β-form creating a purple or red filter pigment (see Zagalsky et al., 1990; Cronin et al., 1994b). This interconversion, with mixing of the two endpoint pigments, is thought to underlie the ability of mantis shrimps to tune the row 3 proximal filters based on the photic environment. Similarly, the row 3 distal 3D-3 filters are apparently formed from a combination of components that have not yet been identified (Cronin et al., 1994b). Similar to the mixing of α- and β-forms of crustacyanin-like pigments in the proximal row 3 filters, mixtures of spectrally different components may also contribute to the tuning of the row 3 distal filters. Whether tuning occurs as in row 2 by varying the incorporation of different filter pigments or in row 3 by varying the composition of mixtures of one or two basic pigments, the selective usage of these pigments permits unusual flexibility in the types of photoreceptor classes used by stomatopods. In particular, the largest diversity of filter classes observed in all filter locations is in the Gonodactyloidea, where species mainly inhabit shallower waters and have evolved visual systems to take advantage of the broad spectrum photic environments in which they live.

## Summary and conclusions

Stomatopod crustaceans rely on a complex and morphologically variable sensory system based on a diversity of photoreceptors and filter pigments not seen elsewhere among animals. In this study we employed methods for examining the patterns of evolution of some of these unusual eye components in order to gain insight into how stomatopods have achieved this visual functional complexity. By reconstructing the ancestral states of visual characters, we have shown that ancestral stomatopod eyes probably contained six midband rows and four filters. Although the earliest lineage contained the most complex eye type observed today, major lineages within the stomatopods have regressively lost diversity in both spectral filters and midband row numbers, with filter loss occurring independently at least three times. This loss of complexity is associated with shifts to less visually complex and/or darker habitats. Perhaps the most intriguing event in the evolution of stomatopod visual systems is the incorporation of spectral filtering of photoreceptors, including the different mechanisms of tuning photoreceptors to the photic environment in midband row 2 *versus* row 3. Whereas midband row 2 proximal filters adapt the underlying photoreceptor to the photic environment by employing a spectrally different filter pigment in each major lineage, both of the midband row 3 filters (proximal and distal) are tunable within an individual

by the flexible interconversion and mixing of different pigments. With respect to filter diversity, the Gonodactyloidea, which inhabit shallow, coral reef habitats, exhibit the largest diversity of classes at all filter locations, allowing them to take advantage of the broad spectrum light available in their environment. Our results illustrate the elaboration of advanced physiological features, providing a unique view of how sensory systems adapt to complex or variable environments.

## LIST OF SYMBOLS AND ABBREVIATIONS

| | |
|---|---|
| aLRT | approximate likelihood ratio test |
| COI | cytochrome oxidase I |
| GTR | general time reversible model |
| ML | maximum likelihood |
| PCR | polymerase chain reaction |
| rDNA | ribosomal DNA |
| R1–R7 | retinular cells 1–7, contained within the main rhabdom of crustacean ommatidia |

## ACKNOWLEDGEMENTS

We would like to thank S. Patek for help in acquiring specimens and two anonymous reviewers for helpful comments on how to improve this manuscript. This study was supported by the Isobel Bennett Marine Biology Fellowship for conducting field work at the Lizard Island Research Station, Queensland, Australia (a facility of the Australian Museum), awarded to M.L.P., and by grants from the National Science Foundation to T.W.C. (IOS0721608) and S. Patek (IOS0641716), and from the Air Force Office of Scientific Research (FA9550-09-1-0149).

## REFERENCES

**Ahyong, S. T.** (1997). A phylogenetic analysis of the Stomatopoda (Crustacea: Malacostraca). *J. Crust. Biol.* **17**, 695-715.
**Ahyong, S. T. and Harling, C.** (2000). The phylogeny of the stomatopod Crustacea. *Austr. J. Zool.* **48**, 607-642.
**Ahyong, S. T. and Jarman, S. N.** (2009). Stomatopod interrelationships: preliminary results based on analysis of three molecular loci. *Arthropod Syst. Phylogeny* **67**, 91-98.
**Anisimova, M. and Gascuel, O.** (2006). Approximate likelihood-ratio test for branches: A fast, accurate, and powerful alternative. *Syst. Biol.* **55**, 539-552.
**Barber, P. H. and Erdmann, M. V.** (2000). Molecular systematics of the Gonodactylidae (Stomatopoda) using mitochondrial cytochrome oxidase C (subunit I) DNA sequence data. *J. Crust. Biol.* **20**, 20-36.
**Barlow, H. B.** (1982). What causes trichromacy? A theoretical analysis using comb-filtered spectra. *Vision Res.* **22**, 635-643.
**Castresana, J.** (2000). Selection of conserved blocks from multiple alignments for their use in phylogenetic analysis. *Mol. Biol. Evol.* **17**, 540-552.
**Cheroske, A. G. and Cronin, T. W.** (2005). Variation in stomatopod (*Gonodactylus smithii*) color signal design associated with organismal condition and depth. *Brain Behav. Evol.* **66**, 99-113.
**Cheroske, A. G., Cronin, T. W. and Caldwell, R. L.** (2003). Adaptive color vision in *Pullosquilla litoralis* (Stomatopoda, Lysiosquilloidea) associated with spectral and intensity changes in light environment. *J. Exp. Biol.* **206**, 373-379.
**Cheroske, A. G., Barber, P. H. and Cronin, T. W.** (2006). Evolutionary variation in the expression of phenotypically plastic color vision in Caribbean mantis shrimps, genus Neogonodactylus. *Mar. Biol.* **150**, 213-220.
**Chiou, T., Kleinlogel, S., Cronin, T., Caldwell, R., Loeffler, B., Siddiqi, A., Goldizen, A. and Marshall, J.** (2008). Circular polarization vision in a stomatopod crustacean. *Curr. Biol.* **18**, 429-434.
**Crandall, K. A. and Fitzpatrick, J. F., Jr** (1996). Crayfish molecular systematics: using a combination of procedures to estimate phylogeny. *Syst. Biol.* **45**, 1-26.
**Cronin, T. W.** (1985). The visual pigment of a stomatopod crustacean, *Squilla empusa*. *J. Comp. Physiol.* **156**, 679-687.
**Cronin, T. W. and Caldwell, R. L.** (2002). Tuning of photoreceptor function in mantis shrimp species occupying a range of depths. II. Filter pigments. *J. Comp. Physiol. A* **188**, 187-197.
**Cronin, T. W. and Marshall, N. J.** (1989a). Multiple spectral classes of photoreceptors in the retinas of gonodactyloid stomatopod crustaceans. *J. Comp. Physiol. A* **166**, 267-275.
**Cronin, T. W. and Marshall, N. J.** (1989b). A retina with at least ten spectral types of photoreceptors in a stomatopod crustacean. *Nature* **339**, 137-140.
**Cronin, T. W. and Marshall, N. J.** (2004). The unique visual world of mantis shrimps. In *Complex Worlds From Simpler Nervous Systems* (ed. F. Prete), pp. 239-268. Cambridge, MA: MIT Press.
**Cronin, T. W., Marshall, N. J. and Caldwell, R. L.** (1994a). The retinas of mantis shrimps from low-light environments (Crustacea; Stomatopoda; Gonodactylidae). *J. Comp. Physiol. A* **174**, 607-619.
**Cronin, T. W., Marshall, N. J. and Caldwell, R. L.** (1994b). The intrarhabdomal filters in the retinas of mantis shrimps. *Vision Res.* **34**, 279-291.
**Cronin, T. W., Marshall, N. J., Caldwell, R. L. and Shashar, N.** (1994c). Specialization of retinal function in the compound eyes of mantis shrimps. *Vision Res.* **34**, 2639-2656.
**Cronin, T. W., Marshall, N. J. and Caldwell, R. L.** (1996). Visual pigment diversity in two genera of mantis shrimps implies rapid evolution. *J. Comp. Physiol. A* **179**, 371-384.
**Cronin, T. W., Caldwell, R. L. and Marshall, J.** (2001). Tunable colour vision in a mantis shrimp. *Nature* **411**, 547-548.
**Cronin, T. W., Caldwell, R. L. and Erdmann, M.** (2002). Tuning of photoreceptor function in mantis shrimp species occupying a range of depths. I. Visual pigments. *J. Comp. Physiol. A* **188**, 179-186.
**Cronin, T. W., Porter, M. L., Bok, M. J., Wolf, J. B. and Robinson, P. R.** (2010). The molecular genetics and evolution of colour and polarization vision in stomatopod crustaceans. *Opthalmic Physiol. Opt.* **30**, 460-469.
**Dowling, T. E., Martasian, D. P. and Jeffery, W. R.** (2002). Evidence for multiple genetic forms with similar eyeless phenotypes in the blind cavefish, *Astyanax mexicanus*. *Mol. Biol. Evol.* **19**, 446-455.
**Folmer, O., Black, M., Hoeh, W., Lutz, R. and Vrijenhoek, R.** (1994). DNA primers for amplification of mitochondrial cytochrome c oxidase subunit I from diverse metazoan invertebrates. *Mol. Mar. Biol. Biotechnol.* **3**, 294-299.
**Gatesy, J., O'Grady, P. and Baker, R. H.** (1999). Corroboration among data sets in simultaneous analysis: hidden support for phylogenetic relationships among higher level artiodactyl taxa. *Cladistics* **15**, 271-314.
**Gillespie, J. J., Johnston, J. S., Cannone, J. J. and Gutell, R. R.** (2006). Characteristics of the nuclear (!8S, 5.8S, 28S and 5S) and mitochondrial (12S and 16S) rRNA genes of *Apis mellifera* (Insecta: Hymenoptera): structure, organization, and retrotransposable elements. *Insect Mol. Biol.* **15**, 657-686.
**Guindon, S. and Gascuel, O.** (2003). A simple, fast, and accurate algorithm to estimate large phylogenies by maximum likelihood. *Syst. Biol.* **52**, 696-704.
**Harling, C.** (2000). Reexamination of eye design in the classification of stomatopod crustaceans. *J. Crust. Biol.* **20**, 172-185.
**Horridge, G. A.** (1978). The separation of visual axes in apposition compound eyes. *Philos. Trans. R. Soc. Lond. B. Biol. Sci.* **888**, 1-59.
**Katoh, K., Misawa, K., Kuma, K. and Miyata, T.** (2002). MAFFT: a novel method for rapid multiple sequence alignment based on fast Fourier transform. *Nucleic Acids Res.* **30**, 3059-3066.
**Katoh, K., Kuma, K., Toh, H. and Miyata, T.** (2005). MAFFT version **5**, improvement in accuracy of multiple sequence alignment. *Nucleic Acids Res.* **33**, 511-518.
**Maddison, W. P. and Maddison, D. R.** (2009). Mesquite: a modular system for evolutionary analysis. Version 2.72 http://mesquiteproject.org.
**Manning, R. B., Schiff, H. and Abbot, B. C.** (1984a). Eye structure and the classification of stomatopod Crustacea. *Zool. Scr.* **13**, 41-44.
**Manning, R. B., Schiff, H. and Abbot, B. C.** (1984b). Cornea shape and surface structure in some stomatopod Crustacea. *J. Crust. Biol.* **4**, 502-513.
**Marshall, N. J.** (1988). A unique colour and polarization vision system in mantis shrimps. *Nature* **333**, 557-560.
**Marshall, J. and Oberwinkler, J.** (1999). Ultraviolet vision: The colorful world of mantis shrimp. *Nature* **401**, 873-874.
**Marshall, N. J., Land, M. F., King, C. A. and Cronin, T. W.** (1991a). The compound eyes of mantis shrimps (Crustacea, Hoplocarida, Stomatopoda). I. Compound eye structure: The detection of polarised light. *Philos. Trans. R. Soc. B. Biol. Sci.* **334**, 33-56.
**Marshall, N. J., Land, M. F., King, C. A. and Cronin, T. W.** (1991b). The compound eyes of mantis shrimps (Crustacea, Hoplocarida, Stomatopoda). II. Colour pigments in the eyes of Stomatopod crustaceans: Polychromatic vision by serial and lateral filtering. *Philos. Trans. R. Soc. B. Biol. Sci.* **334**, 57-84.
**Marshall, N. J., Jones, J. P. and Cronin, T. W.** (1996). Behavioural evidence for color vision in stomatopod crustaceans. *J. Comp. Physiol. A* **179**, 473-481.
**Marshall, N. J., Cronin, T. W. and Kleinlogel, S.** (2007). A review of stomatopod eye structure and function. *Arthropod Struct. Dev.* **36**, 420-448.
**Porter, M. L., Bok, M., Robinson, P. R. and Cronin, T. W.** (2009). Molecular diversity of visual pigments in Stomatopoda (Crustacea). *Vis. Neurosci.* **26**, 255-266.
**Posada, D.** (2008). jModelTest: phylogenetic model averaging. *Mol. Biol. Evol.* **25**, 1253-1256.
**Regier, J. C., Shultz, J. W., Zwick, A., Hussey, A., Ball, B., Wetzer, R., Martin, J. W. and Cunningham, C. W.** (2010). Arthropod relationships revealed by phylogenomic analysis of nuclear protein-coding sequences. *Nature* **463**, 1079-1083.
**Whiting, M. F.** (2002). Mecoptera is paraphyletic: multiple genes and phylogeny of Mecoptera and Siphonaptera. *Zool. Scr.* **31**, 93-104.
**Whiting, M. F., Carpenter, J. C., Wheeler, Q. D. and Wheeler, W. C.** (1997). The Strepsiptera problem: phylogeny of the holometabolous insect orders inferred from 18S and 28S ribosomal DNA sequences and morphology. *Syst. Biol.* **46**, 1-68.
**Zagalsky, P. F., Eilopoulos, E. E. and Findlay, B.** (1990). The architecture of invertebrate carotenoproteins. *Comp. Biochem. Physiol. B Biochem. Mol. Biol.* **97**, 1-18.